



The Abdus Salam  
**International Centre  
for Theoretical Physics**



**2369-18**

**CIMPA/ICTP Geometric Structures and Theory of Control**

*1 - 12 October 2012*

**Hall-MHD and applications**

Daniel Gomez  
*IAFE, Buenos Aires  
Argentina*

# Hall – MHD

## *and applications*

Daniel Gómez <sup>1,2</sup>



Email: [dgomez@df.uba.ar](mailto:dgomez@df.uba.ar)

Webpage: <http://astro.df.uba.ar>

(1) Instituto de Astronomía y Física del Espacio, CONICET, Argentina

(2) Departamento de Física, Universidad de Buenos Aires, Argentina

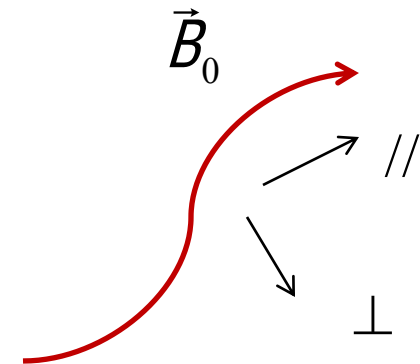


# General Motivation

- Many laboratory, astrophysical and space plasmas can properly be described within the theoretical framework of **Magnetohydrodynamics** (MHD).
- **MHD** is a fluidistic approach to describe the large scale dynamics of plasmas.
- The standard approach is also known as **one-fluid MHD**.
- We are going to start from a somewhat more general approach known as **two-fluid MHD**, which acknowledges the presence of ions and electrons and considers kinetic effects such as **Hall**, **electron pressure** and **electron inertia**.

- Physical processes that can be addressed with MHD include:

- Magnetic reconnection
- Magnetic confinement
- Magnetic dynamo
- MHD turbulence



- We will also address the case of plasmas embedded in strong external magnetic fields, which allow for an approximation known as **reduced MHD**, both for one-fluid MHD (**RMHD**) and two-fluid MHD (**RHMHD**).



# Fluid equations for multi-species plasmas

- For each species  $s$  we have (Goldston & Rutherford 1995):

- Mass conservation 
$$\frac{\partial n_s}{\partial t} + \vec{\nabla} \cdot (n_s \vec{U}_s) = 0$$

- Equation of motion 
$$m_s n_s \frac{d\vec{U}_s}{dt} = q_s n_s (\vec{E} + \frac{1}{c} \vec{U}_s \times \vec{B}) - \vec{\nabla} p_s + \vec{\nabla} \cdot \vec{\sigma}_s + \sum_{s'} \vec{R}_{ss'}$$

- Momentum exchange rate 
$$\vec{R}_{ss'} = -m_s n_s \nu_{ss'} (\vec{U}_s - \vec{U}_{s'})$$

- These moving charges act as sources for electric and magnetic fields:

- Charge density 
$$\rho_c = \sum_s q_s n_s \approx 0$$

- Electric current density 
$$\vec{J} = \frac{c}{4\pi} \vec{\nabla} \times \vec{B} = \sum_s q_s n_s \vec{U}_s$$



# Two-fluid MHD equations

- For a fully ionized plasma with ions of mass  $m_i$  and massless electrons (since  $m_e \ll m_i$ ):

- Mass conservation: 
$$0 = \frac{\partial n}{\partial t} + \vec{\nabla} \cdot (n\vec{U}) \quad , \quad n_e \cong n_i \cong n$$

- Ions: 
$$m_i n \frac{d\vec{U}}{dt} = en \left( \vec{E} + \frac{1}{c} \vec{U} \times \vec{B} \right) - \vec{\nabla} p_i + \vec{\nabla} \cdot \vec{\sigma} + \vec{R}$$

- Electrons: 
$$0 = -en \left( \vec{E} + \frac{1}{c} \vec{U}_e \times \vec{B} \right) - \vec{\nabla} p_e - \vec{R}$$

- Friction force: 
$$\vec{R} = -m_i n \nu_{ie} (\vec{U} - \vec{U}_e)$$

- Ampere's law: 
$$\vec{J} = \frac{c}{4\pi} \vec{\nabla} \times \vec{B} = en (\vec{U} - \vec{U}_e) \quad \Rightarrow \quad \vec{R} = -\frac{m \nu_{ie}}{e} \vec{J}$$

- Polytropic laws: 
$$p_i \propto n^\gamma \quad , \quad p_e \propto n^\gamma$$

- Newtonian viscosity: 
$$\sigma_{ij} = \mu (\partial_i U_j + \partial_j U_i)$$



# Hall-MHD equations

- The dimensionless version, for a length scale  $L_0$ , density  $n_0$  and Alfvén speed  $V_A = B_0 / \sqrt{4\pi m_i n_0}$

$$\frac{d\vec{U}}{dt} = \frac{1}{\varepsilon} (\vec{E} + \vec{U} \times \vec{B}) - \frac{\beta}{n} \vec{\nabla} p_i - \frac{\eta}{\varepsilon n} \vec{J} + \nu \nabla^2 \vec{U}$$

$$\nu = \frac{\mu}{m_i n V_A L_0}$$

$$0 = -\frac{1}{\varepsilon} (\vec{E} + \vec{U}_e \times \vec{B}) - \frac{\beta}{n} \vec{\nabla} p_e + \frac{\eta}{\varepsilon n} \vec{J} \quad \text{where} \quad \vec{J} = \vec{\nabla} \times \vec{B} = \frac{n}{\varepsilon} (\vec{U} - \vec{U}_e)$$

- We define the Hall parameter  $\varepsilon = \frac{c}{\omega_{pi} L_0}$

as well as the plasma beta  $\beta = \frac{\rho_0}{m_i n_0 V_A^2}$  and the electric resistivity  $\eta = \frac{c^2 \nu_{ie}}{\omega_{pi}^2 L_0 V_A}$

- Adding these two equations yields:

$$n \frac{d\vec{U}}{dt} = (\vec{\nabla} \times \vec{B}) \times \vec{B} - \beta \vec{\nabla} (p_i + p_e) + \nu \nabla^2 \vec{U}$$

- On the other hand, using

$$\vec{E} = -\frac{1}{c} \frac{\partial \vec{A}}{\partial t} - \vec{\nabla} \phi$$

$$\vec{B} = \vec{\nabla} \times \vec{A}$$



$$\frac{\partial \vec{A}}{\partial t} = (\vec{U} - \frac{\varepsilon}{n} \vec{\nabla} \times \vec{B}) \times \vec{B} - \vec{\nabla} \phi + \frac{\varepsilon \beta}{n} \vec{\nabla} p_e - \frac{\eta}{n} \vec{\nabla} \times \vec{B}$$

Hall-MHD  
equations



# Hall MHD in a strong field

- Let us assume a strong magnetic field along  $\hat{z}$  so that

$$\vec{B} = \hat{z} + \delta\vec{B} \quad , \quad |\delta\vec{B}| \approx \alpha \ll 1$$

where  $\alpha$  represents the typical tilt of field lines with respect to  $\hat{z}$ . We assume

$$\nabla_{\perp} \approx 1 \quad , \quad \partial_z \approx \alpha \ll 1$$

- The magnetic and velocity fields can be expanded in terms of potentials of order  $\alpha$ :

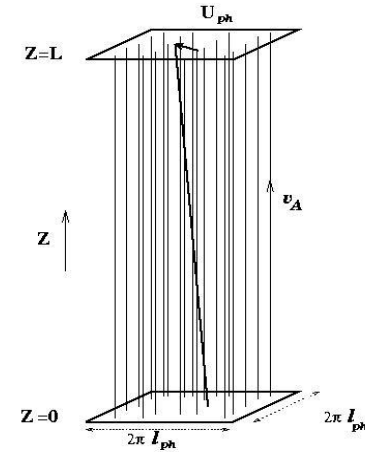
$$\vec{B} = \hat{z} + \vec{\nabla} \times (a\hat{z} + g\hat{x}) = [a_y, -a_x, 1 + b] \quad , \quad b = -g_y$$

$$\vec{U} = \vec{\nabla} \psi + \vec{\nabla} \times (\phi\hat{z} + f\hat{x}) = [\phi_y + \psi_x, -\phi_x + \psi_y, u + \psi_z] \quad , \quad u = -f_y$$

- We want to eliminate the fast scale dynamics, characterized by  $\tau_{A\perp} \approx L_{\perp} / v_A$ , i.e.  $\partial_t \approx 1$

- We obtain the following conditions

$$\begin{aligned} \nabla_{\perp}^2 \psi &= 0 \\ \vec{\nabla}_{\perp} [b + \beta(\rho_i + \rho_e)] &= 0 \\ \vec{\nabla}_{\perp} [\phi + \phi - \varepsilon(b + \beta\rho_e)] &= 0 \end{aligned}$$





# Hall MHD in a strong field

- The relatively slower dynamics, characterized by  $\tau_{A||} \approx L_{||} / V_A$ , i.e.  $\partial_t \approx \alpha$

is given by the following equations (Gomez, Dmitruk & Mahajan 2008):

$$\begin{aligned}
 \partial_t a &= \partial_z(\varphi - \varepsilon b) + [\varphi - \varepsilon b, a] && + \eta \nabla_{\perp}^2 a \\
 \partial_t \omega &= \partial_z j && + [\varphi, \omega] - [a, j] && + \nu \nabla_{\perp}^2 \omega \\
 \partial_t b &= \partial_z(u - \varepsilon j) && + [\varphi, b] + [u - \varepsilon j, a] && + \eta \nabla_{\perp}^2 b \\
 \partial_t u &= \partial_z b && + [\varphi, u] - [a, b] && + \nu \nabla_{\perp}^2 u
 \end{aligned}$$

where  $j = -\nabla_{\perp}^2 a$  and  $\omega = -\nabla_{\perp}^2 \varphi$

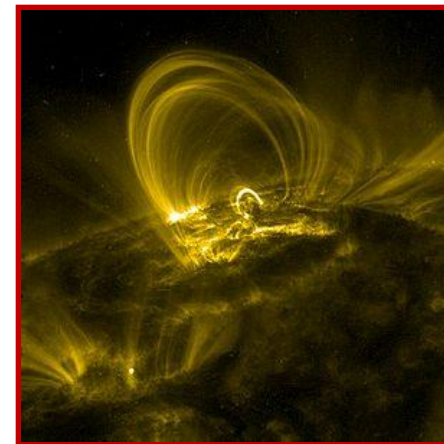
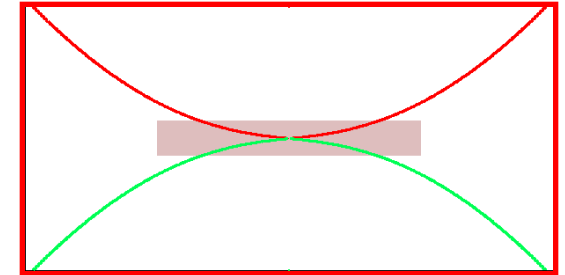
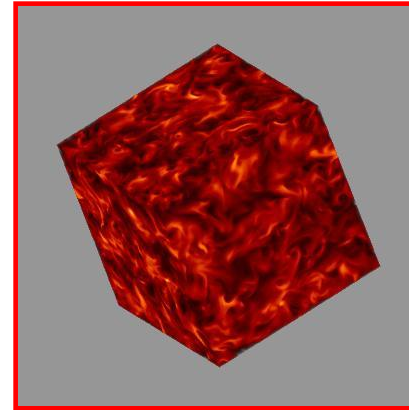
- These are the RHMHD equations. Their ideal invariants (just as for 3D HMHD) are:

$E = \frac{1}{2} \int d^3 r ( \vec{U} ^2 +  \vec{B} ^2) = \frac{1}{2} \int d^3 r ( \vec{\nabla}_{\perp} \varphi ^2 +  \vec{\nabla}_{\perp} a ^2 + u^2 + b^2)$	energy
$H_m = \frac{1}{2} \int d^3 r (\vec{A} \cdot \vec{B}) = \int d^3 r ab$	magnetic helicity
$H_h = \frac{1}{2} \int d^3 r (\vec{A} + \varepsilon \vec{U}) \cdot (\vec{B} + \varepsilon \vec{\Omega}) = \int d^3 r (ab + \varepsilon(a\omega + ub) + \varepsilon^2 u\omega)$	hybrid helicity



# Some applications

- We studied a number of astrophysical problems, within the general framework of MHD:
- 3D Hall-MHD turbulent dynamos.  
(Mininni, Gomez & Mahajan 2003, 2005;  
Gomez, Dmitruk & Mininni 2010)
- 2.5 D Hall-MHD magnetic reconnection in the Earth magnetosphere  
(Morales, Dasso & Gomez 2005, 2006)
- 3D HD helical fluid turbulence  
(Gomez & Mininni 2004)
- RMHD heating of solar coronal loops  
(Dmitruk & Gomez 1997, 1999)
- RHMHD turbulence in the solar wind  
(Martin, Dmitruk & Gomez 2010, 2012)
- Hall magneto-rotational instability in accretion disks  
(Bejarano, Gomez & Brandenburg 2011)





# Simulations

- We integrate the RHMHD eqs. numerically, using a spectral scheme in the perpendicular directions and finite differences along the (much smoother) direction  $z$  (Gomez, Milano and Dmitruk 2000; also Dmitruk, Gomez & Matthaeus 2003)
- We show results from  $512 \times 512 \times 40$  runs performed in (CAPS), our linux cluster with 80 cores
- For the horizontal spatial derivatives, we use a pseudo-spectral scheme with 2/3-dealiasing. Spectral codes are well suited for turbulence studies, since they provide exponentially fast convergence. Spatial derivatives along the loop are computed using finite differences.
- Time integration is performed with a second order Runge-Kutta scheme. The time step is chosen to satisfy the CFL condition. This condition is more stringent if Hall is present, since it displays a quadratic dependence with the grid size.





# Simulations: spatial integration

We focus on **Fourier-Galerkin** methods. Let us illustrate on Burgers equation

$$\partial_t u + u \partial_x u = \nu \partial_{xx} u$$

for  $u(x,t)$  on the interval  $0 \leq x < 2\pi$  assuming periodic boundary conditions and the initial condition  $u(x,0) = u_0(x)$

We expand in a **truncated** Fourier expansion  $\longrightarrow u^N(x,t) = \sum_{k=-N/2}^{N/2} u_k(t) e^{ikx}$

Demanding zero residuals of the solution  $u(x,t)$  when projected on the truncated Fourier space

$$\partial_t u_k = -(u \partial_x u)_k - \nu k^2 u_k, \quad (u \partial_x u)_k = \sum_{l+m=k} i m u_l u_m$$

This truncated expansion  $u^N(x,t)$  **converges exponentially fast** to the exact solution as  $N \rightarrow \infty$

However, it is computationally very demanding, since it involves  $O(N^2)$  operations.



# Simulations: spatial integration

- The **FFT** algorithm yields the discrete set  $\{a_k\}$  from the set  $\{u(x_j)\}$  after  $O(N \log N)$  floating point operations.

$$\{u(x_j), x_j = \frac{2\pi}{N} j, j = 0, \dots, N-1\} \xleftrightarrow{FFT} \{a_k, k = -N/2 + 1, \dots, N/2\}$$

- The strategy of computing spatial derivatives in Fourier space and nonlinear terms in physical space, is known as **pseudo-spectral**, i.e.

$$\partial_t u_k = -(u \partial_x u)_k - \nu k^2 u_k, \quad (u \partial_x u)_k = FFT(FFT^{-1}(u_k) FFT^{-1}(iku_k))$$

- The relation between discrete Fourier coefficients  $\{a_k\}$  and the continuous ones is

$$a_k = u_k + \sum_{m \neq 0} u_{k+Nm}$$

- This sum causes a spurious effect known as **aliasing** when computing nonlinear terms. Aliasing effects can be suppressed by applying the “**two-thirds rule**”, i.e.

$$a_k = 0, \quad \forall |k| \geq N/3$$



# Simulations: temporal integration

- We advance the solution through discrete time steps

$$\longrightarrow t_i = i\Delta t$$

- In compact notation, if

$$\frac{dU}{dt} = F(U, t)$$

where  $F$  is a nonlinear and spatial differential operator, we use a second order **Runge-Kutta** scheme.

- We first advance half a step

$$U^{i+\frac{1}{2}} = U^i + \frac{\Delta t}{2} F(U^i, t_i)$$

and use  $U^{i+\frac{1}{2}}$  to jump the whole step

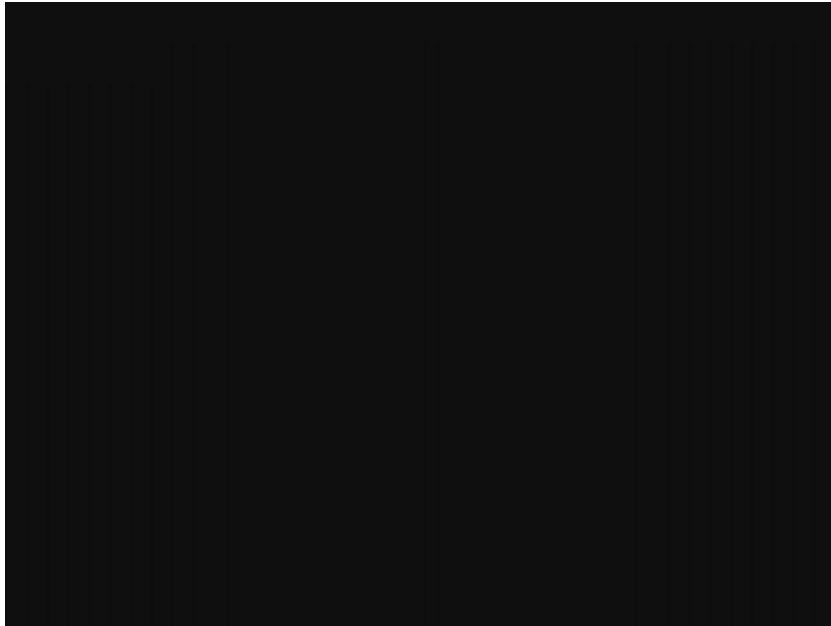
$$\longrightarrow U^{i+1} = U^i + \Delta t F(U^{i+\frac{1}{2}}, t_{i+\frac{1}{2}})$$

- This is second order accurate (i.e.  $O((\Delta t)^2)$ ). The size of the step is limited by the **CFL** condition, i.e.

$$\Delta t \leq \frac{\Delta x}{u_0} \quad \text{for} \quad \partial_t u = u_0 \partial_x u$$



# RMHD applied to coronal loop heating



- The solar corona is a topologically complex array of loops (TRACE movie 171 A)
- Coronal loops are magnetic flux tubes with their footpoints anchored deep in the convective region.
- They confine a tenuous and hot plasma. Typical densities are  $n = 10^9 \text{ cm}^{-3}$  and temperatures are  $T = 2\text{-}3 \cdot 10^6 \text{ K}$ .
- The magnetic field provides not just the confinement of the plasma, but also the energy to heat it up to coronal temperatures ([Parker 1972, 1988](#); [van Ballegoijen 1986](#); [Einaudi et al. 1996](#)).
- One of the key ingredients is the free energy available in the sub-photospheric convective region. Convective motions move the footpoints of fieldlines, thus building up magnetic stresses. See [Mandrini, Demoulin & Klimchuk 2000](#) for a comprehensive comparison between theoretical models and observations for a large number of active regions.
- However, the typical length scale of these magnetic stresses is way too large for the Ohmic dissipation to do the job, since

$$\tau_{diss} \approx l^2 / \eta$$





# RMHD Equations

- Reduced MHD is a self-consistent approximation of the full MHD equations whenever:
  - (a) one component of the magnetic field is much stronger than the others and,
  - (b) spatial variations are smoother along than across (Strauss 1976).

$$\partial_t \mathbf{a} = v_A \partial_z \varphi + [\varphi, \mathbf{a}] + \eta \nabla_{\perp}^2 \mathbf{a}$$

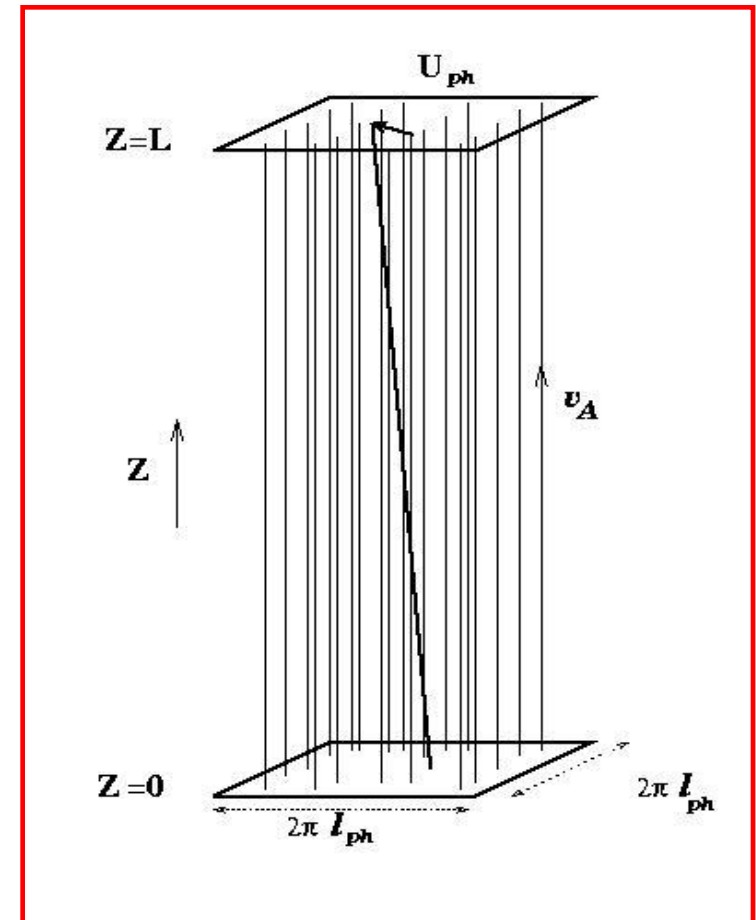
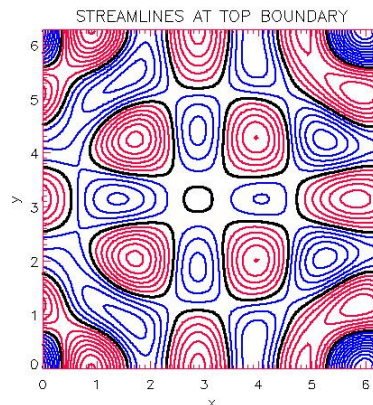
$$\partial_t \omega = v_A \partial_z j + [\varphi, \omega] - [\mathbf{a}, j] + \eta \nabla_{\perp}^2 \omega$$

$$\vec{b} = v_A \hat{z} + \vec{\nabla}_{\perp} \times (\mathbf{a} \hat{z}) \quad , \quad \vec{u} = \vec{\nabla}_{\perp} \times (\varphi \hat{z})$$

$$\omega = -\nabla_{\perp}^2 \varphi \quad , \quad j = -\nabla_{\perp}^2 \mathbf{a}$$

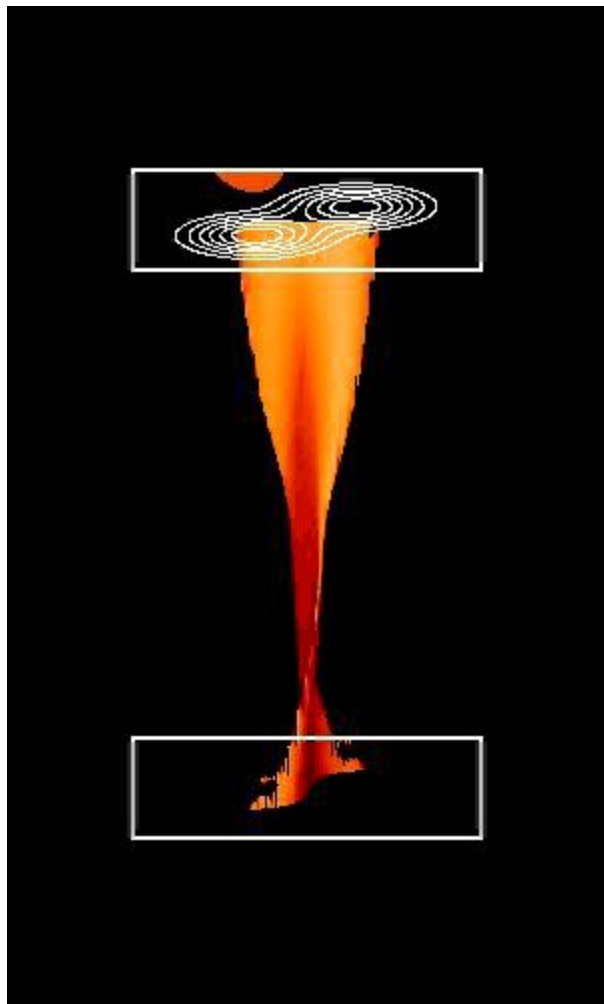
- These equations describe the evolution of the velocity ( $\mathbf{u}$ ) and magnetic field ( $\mathbf{b}$ ) inside the box, assuming periodic boundary conditions at the sides.

- We enforce stationary velocity fields ( $\mathbf{U}_{ph}$ ) at the top plate.





# Current density distribution

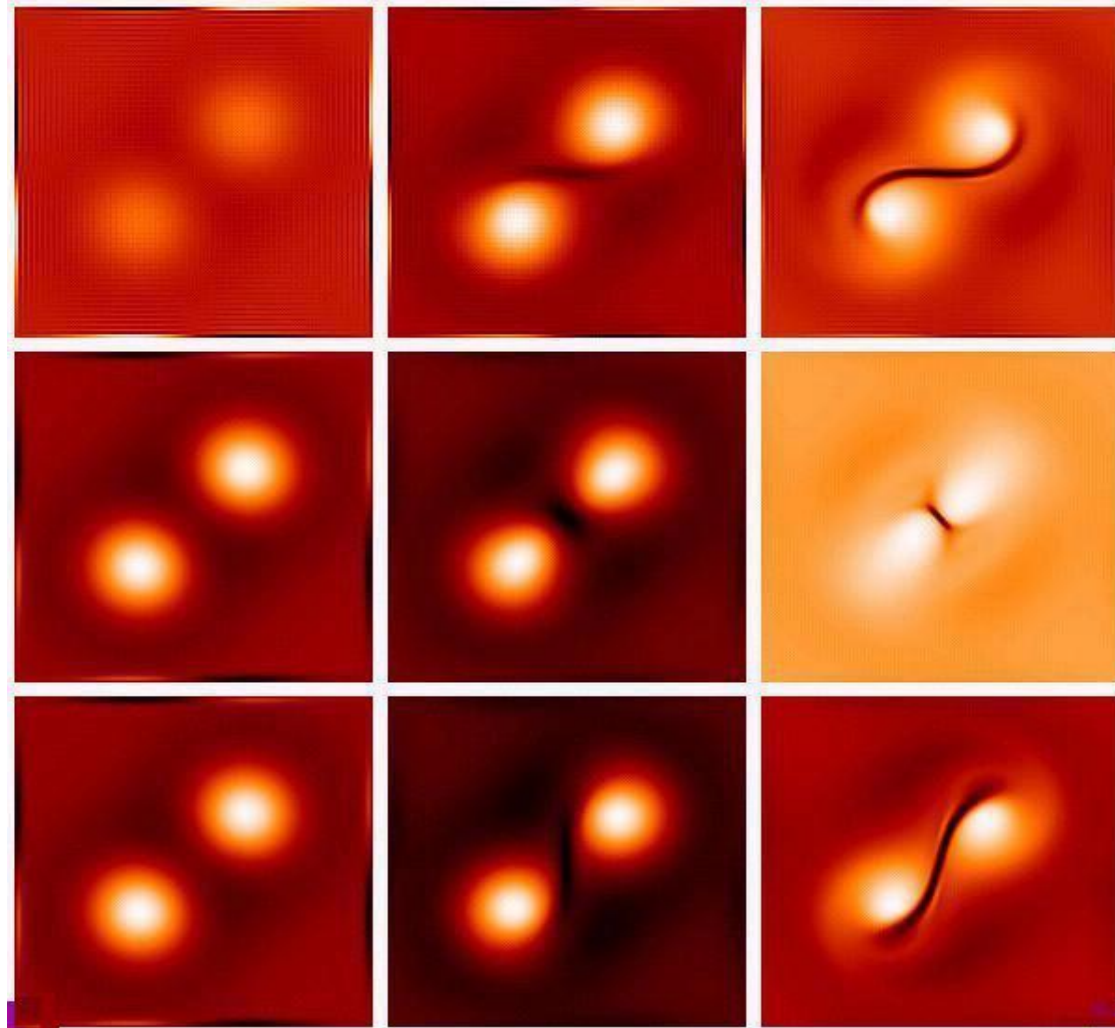


Current density

$Z=0$

$Z=0.5$

$Z=1$



time  $\longrightarrow$

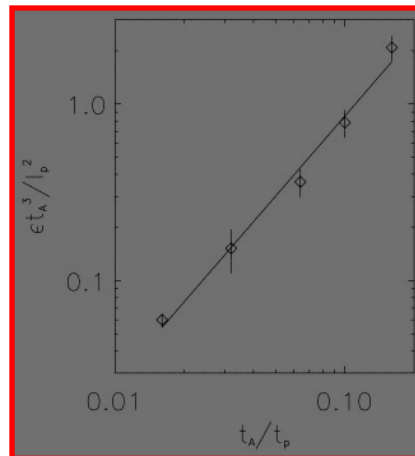




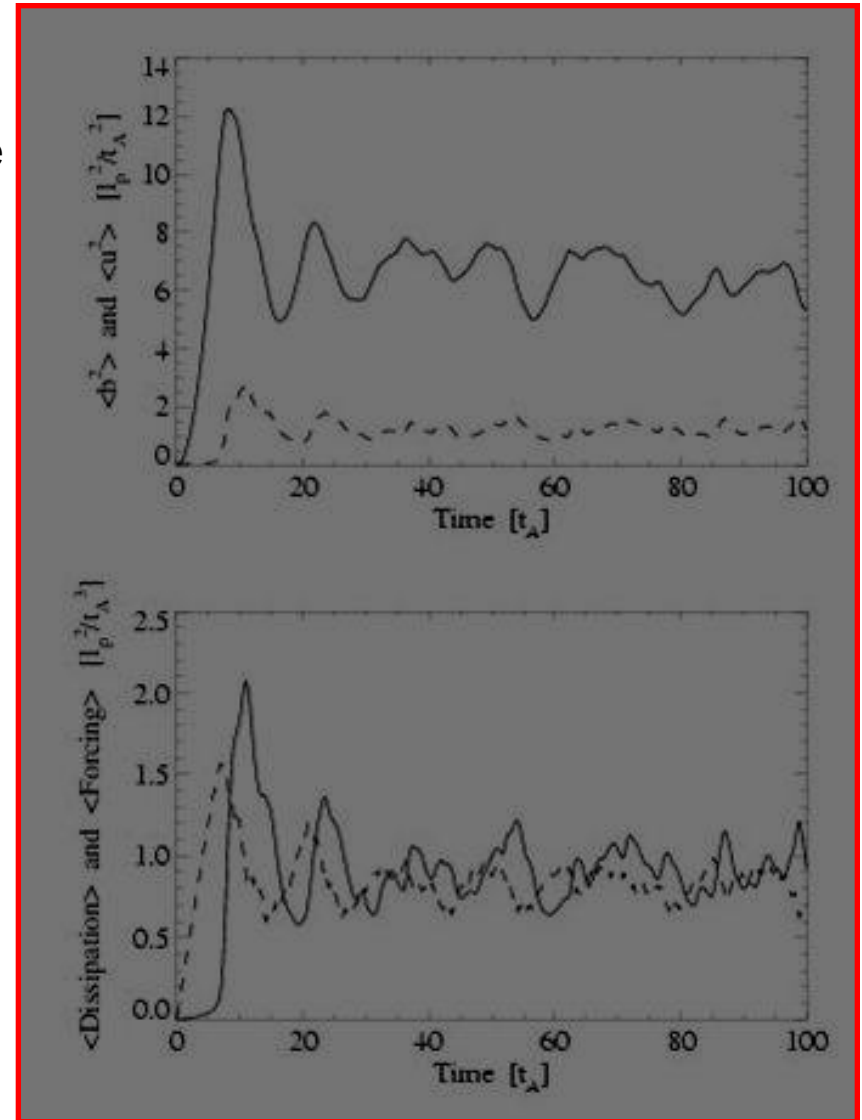
# RMHD simulations

- We perform long time integrations of the RMHD equations. Lengths are in units of the photospheric convective motions ( $\ell_{ph}$ ) and times are in units of the Alfvén time ( $t_A$ ) along the loop.
- Spatial resolution is  $256 \times 256 \times 48$  and the integration time is  $4000 t_A$ . We use a spectral scheme in the  $xy$ -plane and finite differences along  $z$ .
- The time averaged dissipation rate is found to scale like (Dmitruk & Gómez 1999)

$$\varepsilon \approx \frac{\rho \ell_{ph}^2}{t_A^3} \left( \frac{t_A}{t_{ph}} \right)^{3/2}$$



- It is essentially independent of the Reynolds number, as expected for stationary turbulence.





# Stationary turbulence

- Energy cascade
  - energy flux toward high  $k$
  - vortex breakdown

- Scale invariance

- energy flux in  $k$ :

$$\rightarrow \varepsilon_k \approx \frac{U_k^2}{\tau_k}$$

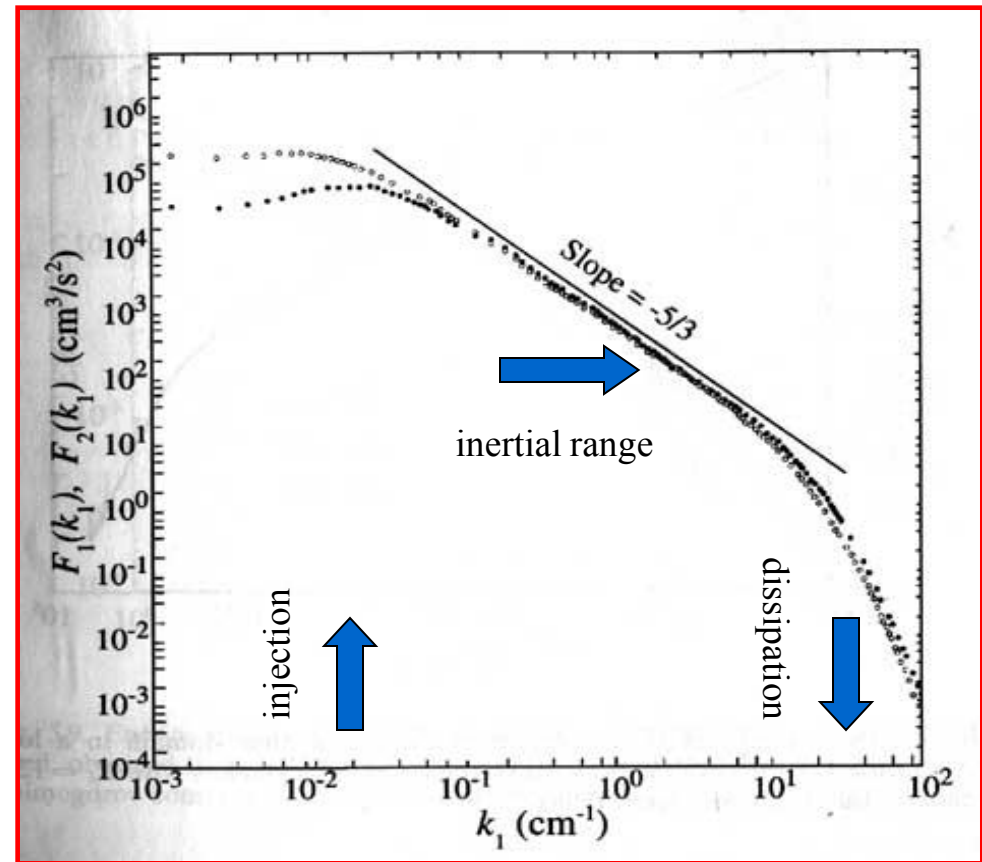
- energy power spectrum:

$$\rightarrow E_k \approx \frac{U_k^2}{k}$$

$$\tau_k \approx \frac{1}{kU_k}, \quad \varepsilon_k \approx \frac{U_k^2}{\tau_k} = \text{const.}$$

- Therefore

$$E_k \approx \frac{U_k^2}{k} = \varepsilon^{\frac{2}{3}} k^{-\frac{5}{3}}$$

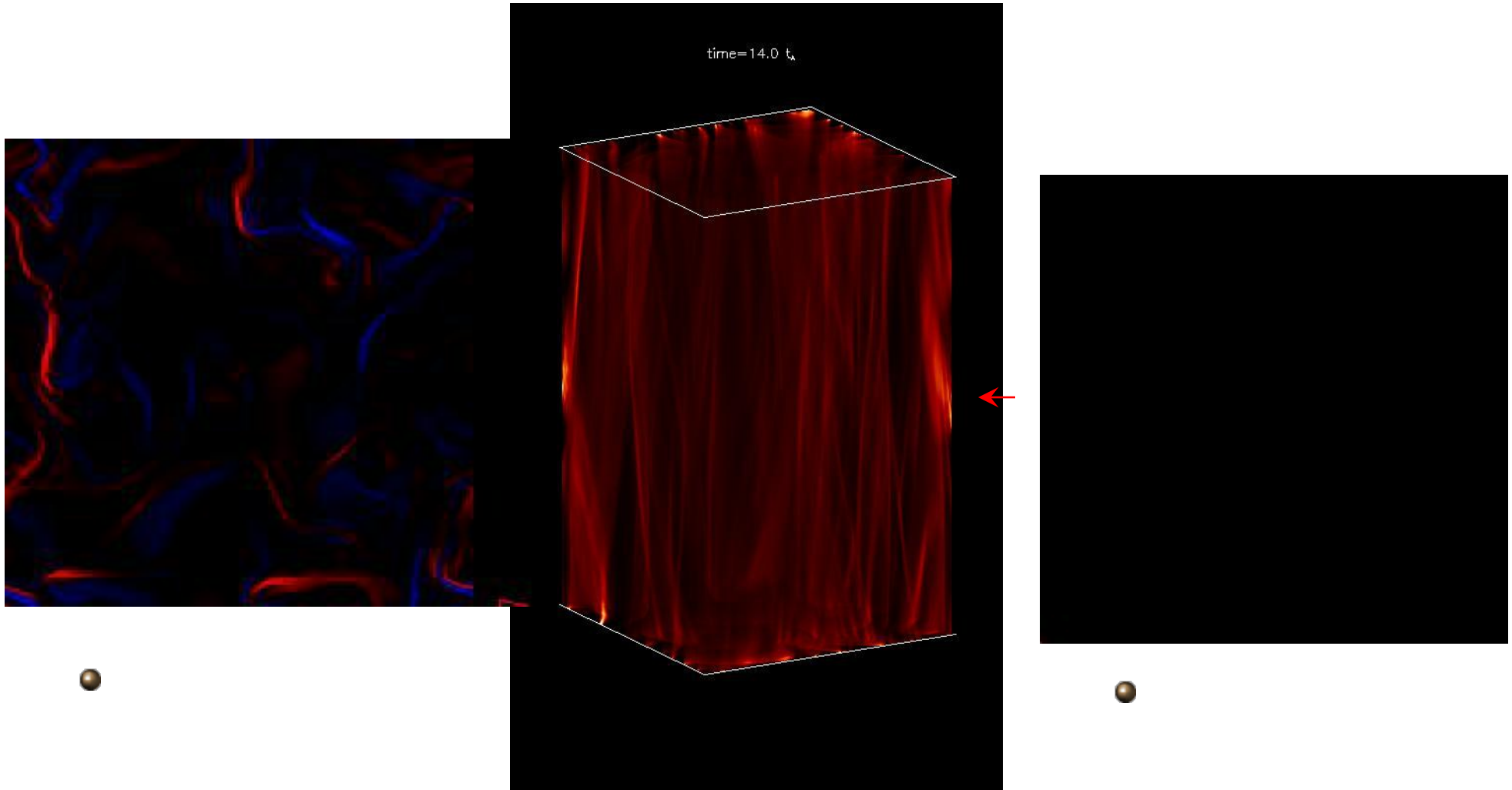


Kolmogorov spectrum (K41)



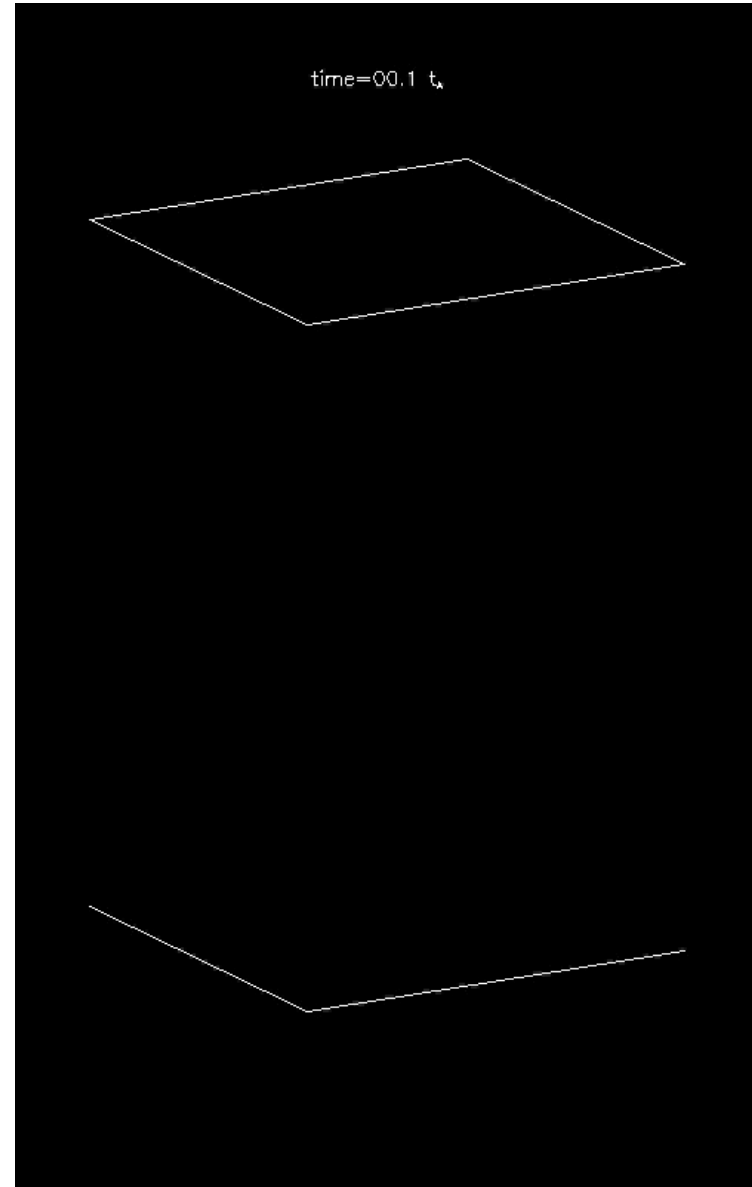
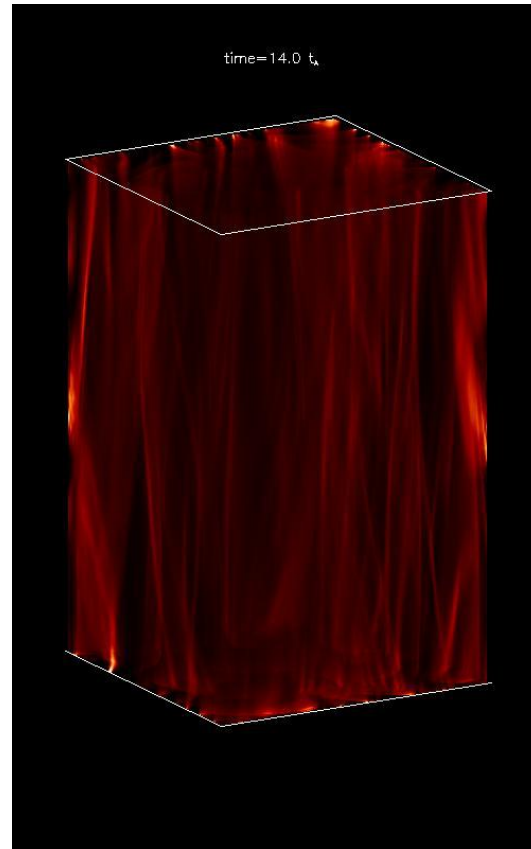
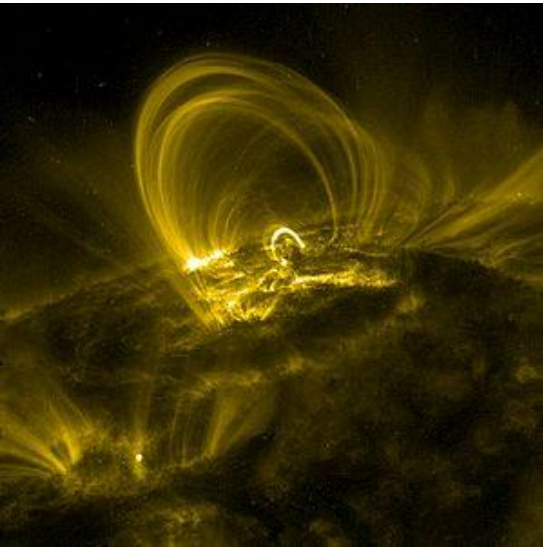
# Dissipative structures: current sheets in 2D

upflows   downflows





# Dissipative structures: current sheets in 3D





# Conclusions

- In this first lecture we introduced the **Hall-MHD** equations, which is an adequate theoretical framework to describe a number of astrophysical and laboratory applications.
- We also presented to so called **reduced** approximation, which is appropriate for plasmas embedded in relatively strong magnetic fields.
- We briefly showed the numerical techniques used to integrate the Hall-MHD equations (spectral and Runge-Kutta).
- As a first application, we showed RMHD simulations (no Hall effect yet) to study the internal dynamics of magnetic loops in the solar corona.
- In the next lecture, we will include the Hall effect and focus on its influence in magnetic reconnection, dynamo mechanisms or turbulence.